

## Quasielastic neutrino scattering: A measurement of the weak nucleon axial-vector form factor

N. J. Baker, A. M. Cnops,\* P. L. Connolly, S. A. Kahn, H. G. Kirk, M. J. Murtagh, R. B. Palmer, N. P. Samios, and M. Tanaka

Brookhaven National Laboratory, Upton, New York 11973

(Received 12 February 1981)

The quasielastic reaction  $\nu_\mu n \rightarrow \mu^- p$  was studied in an experiment using the BNL 7-foot deuterium bubble chamber exposed to the wide-band neutrino beam with an average energy of 1.6 GeV. A total of 1138 quasielastic events in the momentum-transfer range  $Q^2 = 0.06 - 3.00$  (GeV/c)<sup>2</sup> were selected by kinematic fitting and particle identification and were used to extract the axial-vector form factor  $F_A(Q^2)$  from the  $Q^2$  distribution. In the framework of the conventional  $V - A$  theory, we find that the dipole parametrization is favored over the monopole. The value of the axial-vector mass  $M_A$  in the dipole parametrization is  $1.07 \pm 0.06$  GeV, which is in good agreement with both recent neutrino and electroproduction experiments. In addition, the standard assumptions of conserved vector current and no second-class currents are checked.

### I. INTRODUCTION

The electromagnetic structure of the nucleon has been successfully explored using high-energy electrons as probes.<sup>1</sup> An investigation of the corresponding weak structure of the nucleon has been under way for some time via the study of the quasielastic neutrino reaction

$$\nu_\mu n \rightarrow \mu^- p. \quad (1)$$

Most of the experiments have been performed on complex nuclei<sup>2</sup> with one experiment being performed on deuterium.<sup>3</sup> The main purpose of these studies was to measure the weak axial-vector form factor  $F_A(Q^2)$  assuming CVC (conserved vector current) and the absence of second-class currents. This form factor can also be measured via single-pion electroproduction<sup>4</sup> ( $e^- p \rightarrow e^- \pi^+ n$  and  $e^- p \rightarrow e^- \pi^- \Delta^+$ ) using PCAC (partially conserved axial-vector current) and current-algebra-based models. As emphasized by Perkins<sup>5</sup> and more recently by Olsson *et al.*,<sup>6</sup> there appears to be a possible systematic difference in  $F_A(Q^2)$  derived by these two methods: The preferred values of the dipole axial-vector mass from reaction (1) is  $M_A \simeq 0.95$  GeV and from electroproduction is  $M_A \simeq 1.15$  GeV. The importance of obtaining a measurement of this parameter has been recently reemphasized in the analysis of  $\nu p \rightarrow \nu p$  and  $\bar{\nu} p \rightarrow \bar{\nu} p$  scattering and its consequences pertaining to the nature of the basic neutral-current interactions.<sup>7</sup> In this paper we present the results of a study of the quasielastic neutrino reaction (1) observed in the BNL 7-foot deuterium bubble chamber.

### II. EXPERIMENTAL PROCEDURE

The data were obtained from a total of 1 000 000 pictures taken in the BNL 7-foot deuterium bubble chamber exposed to a wide-band neutrino beam

with a mean neutrino energy of 1.6 GeV. A 29-GeV/c proton beam extracted from the AGS struck a sapphire target once every 1.4 sec at the typical intensity of  $\sim 0.8 \times 10^{13}$  protons per pulse. The pions and kaons emerging from the target were focused by a two-horn system and allowed to decay in a 50-m drift space. Muons from  $\pi$  and  $K$  decays were stopped in a 30-m iron filter while the neutrinos passed through to the 7-foot bubble chamber. A sketch of the neutrino-beam layout is shown in Fig. 1.

The bubble chamber is a cylinder 2.1 m (7 ft) in diameter and approximately 3.0 m high and operates in a 25-kG magnetic field. For neutral-current studies, a set of four 1.5-m  $\times$  1.8-m  $\times$  5-cm stainless steel plates were mounted in the downstream region of the chamber as shown in Fig. 2. They were set at an angle of 30° to the beam direction so that they intersected the maximum number of negative tracks. The visible volume with the plates is  $\sim 6$  m<sup>3</sup>.

All pictures were scanned for neutral-induced interactions ( $\geq 2$  prongs) in the chamber. Each event was measured and processed through the TVGP kinematic program, and then reviewed by physicists to check the results of the measurements, visual track identification, and ionization densities. To remove scatters due to incoming charged particles and cosmic neutrons, two cuts were imposed on the basic sample of events: First, the magnitude of the total-visible-momen-

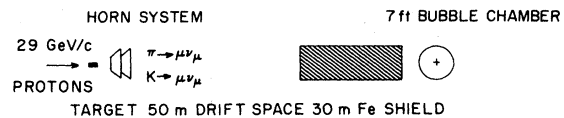


FIG. 1. A schematic diagram of the neutrino beam line and bubble chamber (not to scale).

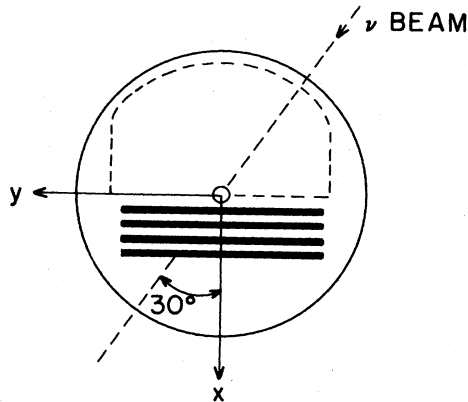


FIG. 2. Top view of bubble chamber with plates and outline of the fiducial volume.

tum vector  $|\vec{P}_{vis}|$  had to be greater than 150 MeV/c and second, the angle between the visible-momentum vector and the beam direction had to be less than  $50^\circ$ . In addition, any event which fitted four-constraint (4C)  $pp \rightarrow pp$  or  $p\pi \rightarrow \pi p$  scattering was rejected. After these cuts, 4480 charged-current (CC) events and 440 neutral-current (NC) candidates were observed. More than 90% of the events are 2- and 3-prong events. All events were kinematically fitted to the appropriate final states. The distributions of the observed neutrino energy and the mass of the hadronic system,  $W$ , for CC events<sup>8</sup> are shown in Figs. 3(a) and 3(b), respec-

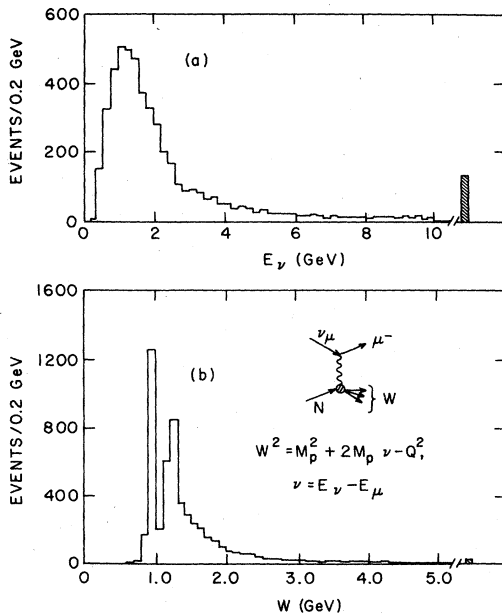


FIG. 3. Distributions of (a) the observed neutrino energy  $E_\nu$ , and (b) the mass of the hadronic system  $W$  for CC events.

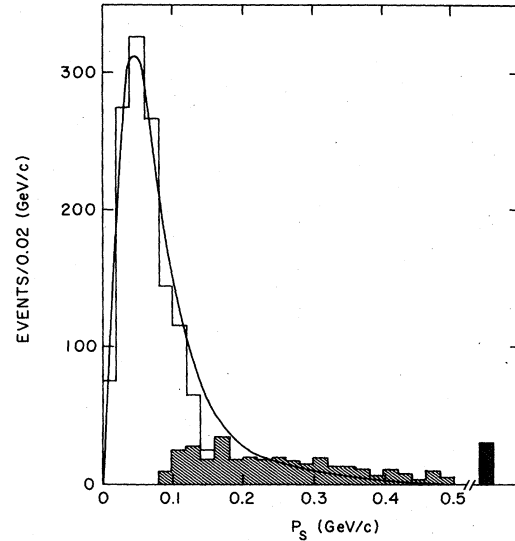


FIG. 4. Spectator momentum distributions for events fitting  $\nu d \rightarrow \mu^- p p_s$ . The cross-hatched area represents the measured spectators. The smooth curve is the prediction of the Hulthén wave function.

tively. The predominant final states are the quasielastic channels  $\mu^- p$  and  $\mu^- \Delta^{++}(1236)$ .

Since the neutrino-beam direction is known to  $\sim 0.5^\circ$ , 3C kinematic fits have been made for the 2- and 3-prong events to the following reactions:



where  $p_s$  and  $n_s$  are the spectator proton and neutron, respectively. If the spectator nucleon was not measurable, the standard bubble-chamber method of assigning an initial value of  $0 \pm 45$  MeV/c for  $p_{x,y,z}$  of the spectator was used. Figure 4 shows the spectator-proton momentum distribution for the events fitting the reaction (2). The shaded areas represent the measured spectator protons. The solid curve is the Hulthén momentum distribution of nucleons in the deuteron which is in agreement with the data.

The quasielastic events are required to fit reaction (2) with a probability  $P(\chi^2) \geq 1\%$ . In addition, the particle identification had to be consistent with the fitted final states (less than 2% of the events are rejected). The large chamber volume, the plates, the trapping power of the high magnetic field, and the relative low momentum of the charged tracks make particle identification possible in a significant sample of the data. In particular,  $\pi^-$ 's are identifiable  $\sim 60\%$  of the time and  $\pi^+$ 's distinguishable from protons  $\sim 80\%$  of the time. This analysis produced 1457  $\nu_\mu d \rightarrow \mu^- p p_s$  events (and 895  $\nu_\mu d \rightarrow \mu^- p \pi^+ n_s$  events). We define

a restricted fiducial volume of 4 m<sup>3</sup> to ensure good event visibility and measurement for the quasielastic events. The outline of the fiducial volume is shown as the dotted line in Fig. 2. The selected events have a minimum distance of 20 cm from the vertex to the first plate or the downstream chamber wall and are seen by all three cameras. Approximately 25% of the events are lost by this fiducial-volume cut. To further reduce possible backgrounds, the following kinematic cuts are made:

- (i)  $\theta_{\text{vis}} < 12^\circ$  and  $M_{\text{X}}^2 \leq 0.5$  (GeV/c)<sup>2</sup>,  
 where  $M_{\text{X}}^2 = (E_{\text{vis}} - M_{\text{tgt}})^2 - \vec{P}_{\text{vis}}^2$ .  
 (ii)  $0.3 \text{ GeV} < E_{\nu} < 6 \text{ GeV}$  and  $\Delta E_{\nu}/E_{\nu} \leq 12\%$ .

After these cuts 1174 events remain.

The mean scanning efficiency determined from a rescan of 30% of the film was 89%. However, it was found not to be uniform over the whole range of  $E_{\nu}$  and  $Q^2$ . A convenient parametrization of this effect was made in terms of  $\cos\theta_{\mu\nu}^*$ , where  $\theta_{\mu\nu}^*$  is the angle in the center of mass of the  $\nu_{\mu} n$  system between the muon and the neutrino direction as shown in Fig. 5. Near  $\cos\theta_{\mu\nu}^* = \pm 1$  the mean efficiency was  $\sim 75\%$  while in the central region  $\cos\theta_{\mu\nu}^* = 0$  was  $\sim 92\%$ . In the calculation of the likelihood functions discussed below, each event was inversely weighted by its scanning efficiency. The use of weighted events affects only the second-class current analysis discussed below.

By examining the 3C  $\nu_{\mu} d \rightarrow \mu^- p \pi^+ n_s$  events and assuming the  $\Delta I = 1$  rule (which experimentally has been shown to be well satisfied), we estimate the background from the reaction  $\nu_{\mu} d \rightarrow \mu^- p \pi^0 p_s$  to be  $(2 \pm 1)\%$ . The background from other sources such as  $\nu_{\mu} d \rightarrow \nu_{\mu} p \pi^+ p_s$  is less than 1%. The con-

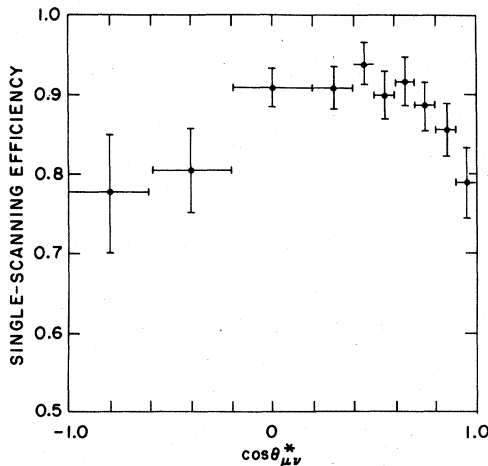


FIG. 5. The single-scanning efficiency as a function of  $\cos\theta_{\mu\nu}^*$ .

tributions to the background from the reaction  $\nu_{\mu} d \rightarrow \mu^- p \pi^+ n_s$  and from non- $\nu$ -induced events are negligible.

### III. FORM-FACTOR ANALYSIS

Assuming locality and the standard  $V-A$  theory, the transition matrix element for the reaction  $\nu_{\mu} n \rightarrow \mu^- p$  can be written as a product of a hadronic weak current and a leptonic current,<sup>9</sup>

$$M = \frac{G}{\sqrt{2}} \cos\theta_C \langle p(p_2) | J_{\lambda}^0 | n(p_1) \rangle \langle \mu(k_2) | \gamma_{\lambda} (1 + \gamma_5) | \nu_{\mu}(k_1) \rangle,$$

where  $G$  is the Fermi constant ( $1.05 \times 10^5 / m_p^2$ ) and  $\theta_C$  is the Cabibbo angle ( $\cos\theta_C = 0.98$ ).  $J_{\lambda}^0$  is the  $\Delta S$  hadronic current

$$J_{\lambda}^0 = \gamma_{\lambda} (F_V^1 + \xi F_V^2) + \frac{q_{\lambda}}{M} F_S - \frac{(p_1 + p_2)_{\lambda}}{2M} \xi F_V^2 \\ + \gamma_{\lambda} \gamma_5 F_A + i \gamma_5 \frac{\sigma_{\mu\nu} q^{\nu}}{M} F_T + \frac{q_{\lambda} \gamma_5}{M} F_P,$$

where  $q = -Q = k_1 - k_2 = p_1 - p_2$ ,  $\xi = \mu_p - \mu_n = 3.708$ , and  $M$  is the nucleon mass. The unknowns in the interaction are the six complex weak nucleon form factors  $F_V^1$  (isovector Dirac),  $F_V^2$  (isovector Pauli),  $F_S$  (induced scalar),  $F_A$  (axial-vector),  $F_P$  (induced pseudoscalar), and  $F_T$  (induced tensor). They are scalar functions of  $Q^2$  only.

In order to simplify the problem, the following standard assumptions are made concerning their transformation properties.

(i) Time-reversal invariance and charge symmetry. As a consequence, all form factors are real and no second-class currents exist ( $F_S = F_T = 0$ ).

(ii) For the small induced pseudoscalar term PCAC is assumed. Then  $F_P$  is dominated by the pion pole and given by

$$F_P(Q^2) \approx 2M^2 F_A(Q^2) / (Q^2 + m_{\pi}^2).$$

The contribution to the cross section from this term is less than 2%.

(iii) Isotriplet-vector-current hypothesis (CVC). If CVC is valid, then  $F_S = 0$ , and  $F_V^1$  and  $F_V^2$  are related to the isovector Sachs electric and magnetic form factors  $G_E^V$  and  $G_M^V$  obtained from electron scattering experiments as follows:

$$G_E^V(Q^2) = F_V^1(Q^2) + Q^2 / 4M^2 \xi F_V^2(Q^2),$$

$$G_M^V(Q^2) = F_V^1(Q^2) + \xi F_V^2(Q^2).$$

To an accuracy of 5% these form factors are adequately represented by the dipole form and the "scaling" relation,

$$G_E^V(Q^2) = G_M^V(Q^2) / (1 + \xi) = \lambda(Q^2) / (1 + Q^2 / M_V^2)^2,$$

where  $M_V$  is the vector mass and  $\lambda(Q^2)$  is a small

correction factor for the deviations of the electron scattering data from a pure dipole form factor (if CVC is correct,  $M_V = 0.84$  GeV).<sup>6,10</sup>

(iv) We further assume the dipole form for the axial-vector form factor

$$F_A(Q^2) = F_A(0)/(1 + Q^2/M_A^2)^2,$$

where the value of  $F_A(0) = -1.23 \pm 0.01$  is taken from  $\beta$  decay and  $M_A$  is the axial-vector mass. With these assumptions the only unknown parameter is  $M_A$ .

The differential cross section for the reaction (1) can be written as<sup>9</sup>

$$\frac{d\sigma}{dQ^2} = \frac{G^2 M^2 \cos^2 \theta_C}{8\pi E_\nu^2} [A(Q^2) + B(Q^2)W + C(Q^2)W^2], \quad (4)$$

where

$$Q^2 = 2E_\nu(E_\mu - p_\mu \cos \theta_{\mu\nu}),$$

$$W = E_\nu/M - Q^2/4M^2 - m_\mu^2/4M^2,$$

and the structure functions  $A$ ,  $B$ , and  $C$  are functions of  $Q^2$ :

$$\begin{aligned} A &= \frac{Q^2}{4M^2} \left[ \left(4 + \frac{Q^2}{M^2}\right) |F_A|^2 - \left(4 - \frac{Q^2}{M^2}\right) |F_V^2|^2 \right. \\ &\quad \left. + \frac{Q^2}{M^2} \left(1 - \frac{Q^2}{4M^2}\right) |\xi F_V^2|^2 \right. \\ &\quad \left. + \frac{4Q^2}{M^2} \operatorname{Re} F_V^{1*} F_V^2 - \frac{Q^2}{M^2} \left(4 + \frac{Q^2}{M^2}\right) |F_T|^2 \right], \\ B &= -\frac{4Q^2}{M^2} \operatorname{Re} F_A^*(F_V^1 + \xi F_V^2), \quad (5) \\ C &= 4 \left( |F_A|^2 + |F_V^1|^2 + \frac{Q^2}{4M^2} |\xi F_V^2|^2 + \frac{Q^2}{4M^2} |F_T|^2 \right). \end{aligned}$$

At low energies  $E_\nu \sim 1$  GeV, the contributions to the cross section from  $A$ ,  $B$ , and  $C$  are the same order of magnitude. Therefore, we can get the maximum information on the form factors.

We have used a maximum likelihood method to extract  $M_A$  from the shape of the  $Q^2$  distribution for each observed neutrino energy. This likelihood function  $\mathcal{L}^f$  is independent of the shape of the neutrino spectrum and is defined by

$$\mathcal{L}^f = \prod_{i=1}^N \frac{(d\sigma/dQ^2)(Q_i^2, E_\nu^i, M_A, M_V) R(Q_i^2)}{\int_{Q_{\min}^2}^{Q_{\max}^2} (d\sigma/dQ^2)(Q_i^2, E_\nu^i, M_A, M_V) R(Q_i^2) dQ^2},$$

where  $N$  is the total number of selected events and  $R(Q^2)$  is a correction factor for the cross section due to the deuteron effects, the Pauli exclusion principle, and the effect of the Fermi motion.<sup>11</sup> The ratio  $R(Q^2)$ , which is defined as  $\sigma(\nu_\mu d - \mu^- p p_s) / \sigma(\nu_\mu n - \mu^- p)$ , is neither sensitive to  $E_\nu$  nor to the choice of form factors but depends strongly on  $Q^2$  at  $Q^2 \lesssim 0.2$  (GeV/c)<sup>2</sup>.

A loss of events at  $Q^2 \approx 0$  is expected because such events have a low-momentum recoil proton and will appear as 1-prong events. To avoid a bias from this loss, a cut has been imposed on the data at  $Q_{\min}^2 = 0.06$  (GeV/c)<sup>2</sup>, which corresponds to a proton range  $\sim 6.8$  cm (or  $p \sim 250$  MeV/c) in the bubble chamber. After this cut 1138 events (1236 weighted events) are left for analysis.

#### IV. RESULTS AND DISCUSSION

With the standard assumptions described above and a fixed value of  $M_V = 0.84$  GeV, a one-parameter fit to the data gives  $M_A = 1.07 \pm 0.06$  GeV for the dipole form of  $F_A$ . If we fit the data with a monopole form or a QM-VD (quark-model-vector-dominance) form<sup>12</sup>

$$F_A(Q^2) = F_A(0)(1 + Q^2/M_A^2)^{-1} \exp[-\frac{1}{8} Q^2 R^2 / (1 + Q^2/4M^2)],$$

where  $R^2 = 6$  GeV<sup>-2</sup>, then we find that the best values of  $M_A^{\text{monopole}} = 0.57 \pm 0.05$  GeV and  $M_A^{\text{QM-VD}} = 1.31 \pm 0.16$  GeV, respectively. The errors correspond to a change in the likelihood functions by 0.5 units. However, the monopole form can be excluded at the level of 3.8 standard deviations, based on the values of the likelihood functions. One should note that the value of  $M_A^{\text{QM-VD}}$  is in good agreement with the mass of the  $A_1$  meson. In Fig. 6 we show the  $Q^2$  distribution for the selected events with the theoretical prediction for  $M_A = 1.07$  GeV (the solid line). There is good agreement with the data. Figure 7 shows the relative  $\nu_\mu$  flux spectrum obtained from the observed  $E_\nu$  distribu-

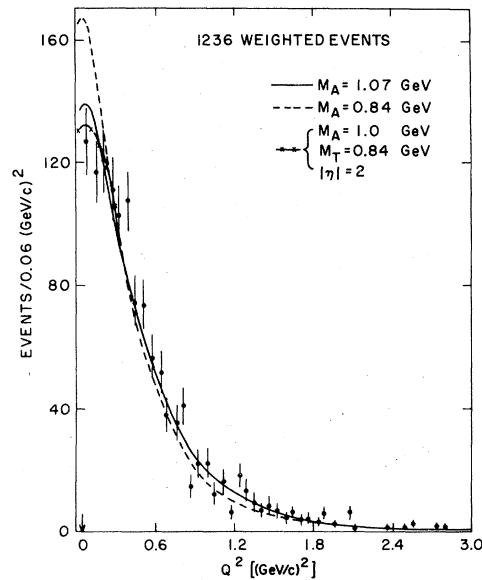


FIG. 6. The  $Q^2$  distribution for selected quasielastic events. The smooth line shows the best fit for  $M_A = 1.07$  GeV.

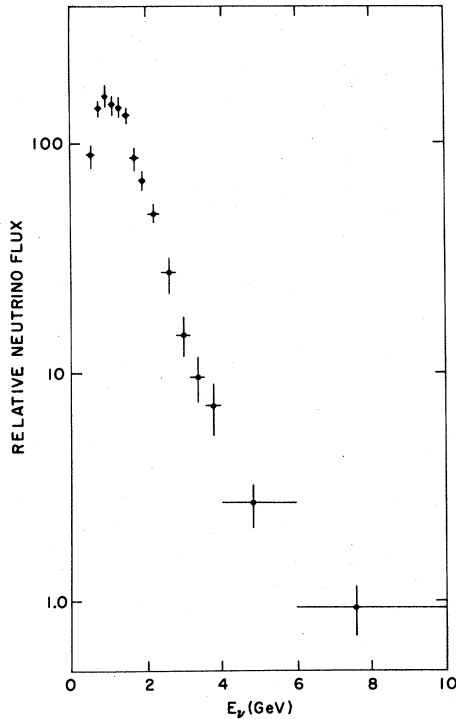


FIG. 7. The relative  $\nu_\mu$  flux spectrum obtained from the observed  $E_\nu$  distribution of the events with  $M_A = 1.07$  GeV.

tion of the events after correcting for the deuteron effects and the  $Q_{\min}^2$  cut.

The systematic effects have been studied by checking variations of the fitted  $M_A$  values against changes in the selection criteria such as inclusion of background events, cuts on event topology,  $Q_{\min}^2$ ,  $P(\chi^2)$ , etc. In every case the results are consistent within the errors, indicating that the systematic errors are small compared with the quoted errors. Figure 8 shows the fitted  $M_A$  values for various minimum  $Q^2$  cuts and it illustrates that with the minimum  $Q^2$  cut,  $Q_{\min}^2 = 0.06$   $(\text{GeV}/c)^2$ , there is no apparent bias due to scanning and/or measuring biases for events with low-momentum protons.

In Fig. 9 the previous measurements of  $M_A$  from neutrino experiments are shown.<sup>2,3</sup> The value obtained in this experiment is consistent with, but somewhat higher than, the previous world average for  $M_A$ . The result is also consistent with the results from electroproduction experiments. The value of  $M_A$  obtained is 3.6 standard deviations from the equality  $M_A = M_\nu = 0.84$  GeV and is, in fact, closer to the theoretically suggested value  $M_A = \sqrt{2} M_\nu$ .<sup>13</sup>

The results given above are based on the "conventional" assumptions of CVC, no second-class

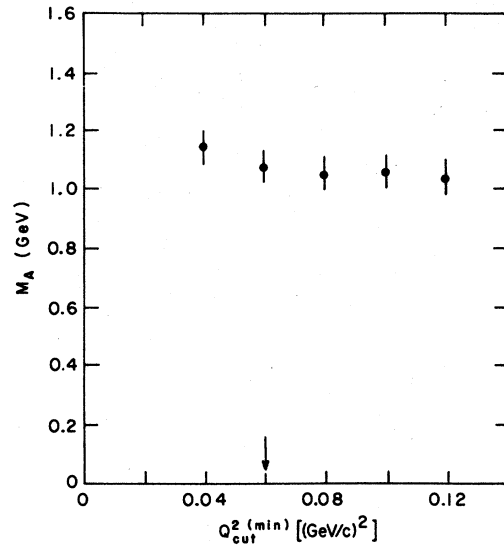


FIG. 8.  $M_A$  for various  $Q_{\min}^2$  cuts.

currents, and a PCAC-predicted induced pseudo-scalar term. We now address the experimental evidence for the validity of these assumptions. Firstly, we can perform a two-parameter fit where both  $M_A$  and  $M_\nu$  are allowed to vary. Such a fit yields  $M_A = 1.04 \pm 0.14$  GeV and  $M_\nu = 0.86 \pm 0.07$  GeV which is in excellent agreement with the CVC value of  $M_\nu = 0.84$  GeV which had been used in the one-parameter fits.

Secondly, we can look for any neutrino-energy

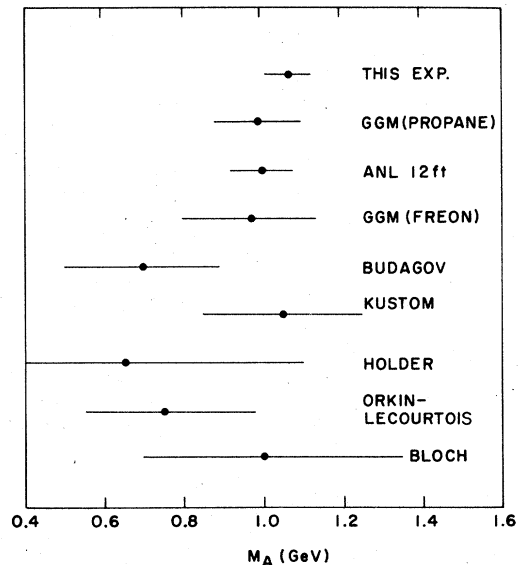


FIG. 9. A comparison of value of  $M_A$  determined in this experiment and values obtained by previous neutrino experiments.

TABLE I. Measurement of  $M_A$  as a function of  $E_\nu$ .

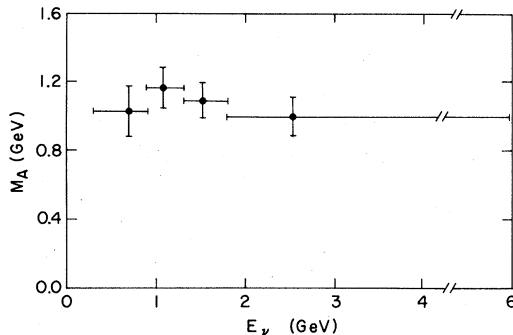
$E_\nu$ (GeV)	$\langle E_\nu \rangle$ (GeV)	Number of events <sup>a</sup>	$M_A$ (GeV)
0.3–0.9	0.69	256 (275)	$1.03 \pm 0.15$
0.9–1.3	1.08	302 (326)	$1.17 \pm 0.12$
1.3–1.8	1.52	295 (319)	$1.08 \pm 0.10$
1.8–6.0	2.55	285 (316)	$1.00 \pm 0.11$
0.3–6.0	1.48	1138 (1236)	$1.070 \pm 0.057$

<sup>a</sup> The numbers in parentheses are the weighted numbers of events.

dependence in the determined values of  $M_A$  should be independent of the neutrino energy.<sup>14</sup> Table I and Fig. 10 show results of analyses performed using four different regions of energy. The results are very consistent with the value of  $M_A = 1.07$  GeV. Another, and more sensitive, analysis comes for the observation that the energy dependence of the data is of a quadratic form [Eq. (4)] which allows, in principle,  $M_A$  to be determined independently from the three structure functions  $A(q^2)$ ,  $B(q^2)$ , and  $C(q^2)$  [see Eq. (5)]. Performing such an analysis gives  $M_A^{(A)} = 0.78 \pm 0.37$ ,  $M_A^{(B)} = 0.92 \pm 0.14$ , and  $M_A^{(C)} = 1.34 \pm 0.13$  GeV. The differences in these values, although not very significant, do suggest a possible violation of the assumptions. It should be noted from Eq. (5) that a second-class current appears in term  $C$  multiplied by  $Q^2$ , has a small effect on  $B$ , and appears in  $A$ , again multiplied by  $Q^2$ , but with a sign opposite to that in term  $C$ . Consequently, the presence of a second-class current with form similar to  $F_A$  (due to the extra  $Q^2$  factor) would raise the apparent  $M_A^{(C)}$ , have little effect on  $M_A^{(B)}$ , and decrease  $M_A^{(A)}$ . This is the trend observed in the second analysis. Following this lead we can analyze the data allowing a second-class current of the form

$$F_T(Q^2) = \eta F_A(0) / (1 + Q^2/M_T^2)^2.$$

When such a term is included the analysis be-

FIG. 10.  $M_A$  as a function of  $E_\nu$ .

comes more complicated. In principle, one must simultaneously fit  $M_A$ ,  $M_T$  and  $\eta$ , but the data are not sufficient to allow meaningful values to be obtained for these three parameters simultaneously. It is found, however, that for any reasonable value of  $M_T$  a finite value of  $\eta$  is preferred. For instance, one obtains  $M_A = 1.1 \pm 0.1$  GeV and  $|\eta| = 3 \pm 1$  for  $M_T = 0.84$  GeV, and  $M_A = 1.0 \pm 0.1$  GeV and  $|\eta| = 1.2 \pm 0.6$  for  $M_T = 1.05$  GeV.

We have examined the predicted distributions in  $Q^2$  and  $E_\nu$  in order to determine the nature of the possible signal requiring the second-class current in the fit. A pronounced difference is revealed if the data are studied using the variable  $\cos\theta_{\bar{\nu}\nu}^*$ . It is found that a second-class current enhances the central region of the  $\cos\theta_{\bar{\nu}\nu}^*$  distribution and suppresses both high and low values. It was for this reason that the scanning efficiency was determined as a function of this variable.

As has been noted above, the scanning efficiency was not dependent of this variable, but did indeed peak in the center and fall towards the ends (see Fig. 5). We have attempted to correct for this effect by weighting the events as a function of  $\cos\theta_{\bar{\nu}\nu}^*$ . If this correction is not made then the apparent second-class signal is even larger than given above. The question we must now address is whether the remaining signal is real or a further sensitive reflection of a scanning bias. At present the cause of the variation in  $\cos\theta_{\bar{\nu}\nu}^*$  is not fully understood. Further, the determination of the bias of the double-scan method presupposes no correlation between the two scans, something that is not the case here. It is not unreasonable therefore to assume that the bias is only partially corrected by our procedure and the remaining apparent second-class signal is still an effect of the bias.

A final attempt to remove the bias involves selecting events where the azimuthal angle of the proton is within  $45^\circ$  of the horizontal, i.e., selecting events that lie in planes more nearly perpendicular to the camera view where the scanning efficiency should be better. When this is done the best fit gives  $M_A = 1.0 \pm 0.1$  GeV and  $|\eta| = 0.8 \pm 0.7$  for  $M_T = 1.05$  GeV, and  $M_A = 1.1 \pm 0.1$  GeV and  $|\eta| = 2 \pm 1$  for  $M_T = 0.84$  GeV with a significance determined from the confidence level of 0.6 and 1.2 standard deviations, respectively. It is clear that we do not have a significant indication of a second-class current.

If this final data sample is used to set an upper limit on the second-class current then, with  $M_A \approx M_T \approx M_N$ , where  $M_N$  is the nucleon mass, we obtain

$$|\eta| \leq 2.0 \text{ (90\% C. L.)}$$

## V. CONCLUSION

The quasielastic reaction  $\nu n \rightarrow \mu \bar{p}$  has been examined with good statistics and understanding of systematics. This has been accomplished via the utilization of a large bubble chamber, using deuterium as a target, and employing a large exposure of  $10^6$  pictures. From a total sample of 5000 charged-current neutrino events,  $\approx 1500$  quasielastic events were observed, of which 1138 occurred in a restricted fiducial volume. Owing to the excellent geometrical trapping power and spatial resolution of the chamber, the events are essentially uniquely identified. Examination of the energy  $E_\nu$  and momentum transfer  $Q^2$  distribution of these events affords the opportunity of performing an analysis of the weak structure functions of the hadrons. The standard analysis procedure yields a value for the axial-vector mass (in a dipole parametrization),  $M_A = 1.07 \pm 0.06$  GeV, this number being stable under application of a variety of cuts.  $M_A$  is therefore larger than  $M_V = 0.84$  GeV, the vector mass. The value found in this experiment,  $M_A = 1.07$  GeV, is consistent with both previous neutrino measurements (Fig. 9) and electroproduction measurements.

Attempts to delineate the detailed structure of

the weak hadronic current have been less successful. Attempts were made to see if there were terms beyond the accepted vector and axial-vector forms. These proved inconclusive. Some indications of the possible existence of second-class currents were indicated by the data at the  $2.5\sigma$  level. It was determined that a scanning bias as determined from a double scan of the film was not sufficient to explain it all. When events are restricted to lie in planes more perpendicular to the camera axis, i.e., so that they are more clearly visible, the indication for second-class currents disappears. A new  $10^6$ -picture exposure in deuterium has recently been taken. The analysis is expected to be completed in approximately one year, whereupon further light can be shed on this important question.

## ACKNOWLEDGMENTS

We are grateful to the 7-foot bubble-chamber crew, to Ms. Fern M. Coyle who helped in the editing, and to the scanning-measuring personnel at BNL for their dedicated efforts. This research was supported by the U.S. Department of Energy under Contract No. DE-AC02-76CH00016.

\*Present Address: DD Division, CERN, Geneva, Switzerland.

<sup>1</sup>C. de Varies *et al.*, Phys. Rev. Lett. **8**, 381 (1962).

<sup>2</sup>M. M. Bloch *et al.*, Phys. Lett. **12**, 281 (1964); A. Orkin-Lecourtois and C. A. Piketty, Nuovo Cimento **50A**, 927 (1967); M. Holder *et al.*, *ibid.* **47A**, 338 (1968); R. L. Kustom *et al.*, Phys. Rev. Lett. **22**, 1014 (1969); I. Budagov *et al.*, Lett. Nuovo Cimento **2**, 689 (1969); S. Bonetti *et al.*, Nuovo Cimento **38A**, 260 (1977) [GGM (freon)]. See also, M. Dewit, in *Proceedings of the Topical Conference on Neutrino Physics at Accelerators, Oxford, 1978*, edited by A. Michette and P. Renton (Rutherford Laboratory, Chilton, Didcot, Oxfordshire, England, 1978), p. 75 [GGM (propane)].

<sup>3</sup>W. A. Mann *et al.*, Phys. Rev. Lett. **31**, 844 (1973); S. J. Barish *et al.*, Phys. Rev. D **16**, 3103 (1977) [ANL (12 ft)].

<sup>4</sup>E. Amaldi *et al.*, Phys. Lett. **41B**, 216 (1972); E. D. Bloom *et al.*, Phys. Rev. Lett. **30**, 1186 (1973); P. Branel *et al.*, Phys. Lett. **45B**, 386 (1973); A. del Geurra *et al.*, Nucl. Phys. **B107**, 65 (1976); P. Joos *et al.*, Phys. Lett. **62B**, 230 (1976).

<sup>5</sup>D. H. Perkins, in *Proceedings of the International Symposium on Lepton and Photon Interactions at High Energies, Stanford, California, 1975*, edited by W. T.

Kirk (SLAC, Stanford, 1976).

<sup>6</sup>M. G. Olsson *et al.*, Phys. Rev. D **17**, 2938 (1978).  $\lambda(Q^2)$  is defined by  $\lambda^2(Q^2) = 1 - (0.053 + 0.017Q) \sin [4Q/(1 + 0.220)]$  for  $Q^2 \lesssim 6$  (GeV/c)<sup>2</sup>, where  $Q = \sqrt{Q^2}$ .

<sup>7</sup>D. P. Sidhu and P. Langacker, Phys. Rev. Lett. **41**, 732 (1978); M. Claudson *et al.*, Phys. Rev. D **19**, 1373 (1979); E. A. Paschos, *ibid.* **19**, 83 (1979).

<sup>8</sup>To obtain the neutrino energy and  $W$ , the event was calculated on the assumption of its being a single neutral ( $n$  or  $\pi^0$ ) if the kinematics indicated one or more neutrals were missing.

<sup>9</sup>See, for example, R. E. Marshak, Riazuddin, and C. P. Ryan, *Theory of Weak Interactions in Particle Physics*, (Wiley-Interscience, New York, 1969); C. H. Llewellyn-Smith, Phys. Rep. **3C**, 261 (1972).

<sup>10</sup>B. Bartoli *et al.*, Riv. Nuovo Cimento **2**, 2411 (1972).

<sup>11</sup>S. K. Singh, Nucl. Phys. **B36**, 419 (1971).

<sup>12</sup>L. M. Sehgal, in *Proceedings of the International Conference on High-Energy Physics, European Physical Society, Geneva, 1979*, edited by A. Zichichi (CERN, Geneva, Switzerland, 1979), p. 98.

<sup>13</sup>S. Weinberg, Phys. Rev. Lett. **18**, 507 (1967).

<sup>14</sup>V. A. Korotkov *et al.*, Yad. Fiz. **26**, 601 (1977) [Sov. J. Nucl. Phys. **26**, 318 (1977)].